

RESEARCH ARTICLE

Navier-Stokes- ω model with slip and friction boundary conditions at high Reynolds numbers

Ö. İlhan

Department of Mathematics, Faculty of Science, Mugla Sıtkı Kocman University, 48050, Mugla, Turkey
 Phone: +902522111506; Fax: +902522111472

ABSTRACT - The no-slip boundary condition is indeed a fundamental concept in fluid dynamics, especially for flows at lower Reynolds numbers (Re) where viscous effects dominate. However, inertial effects become more significant at higher Reynolds numbers, and the no-slip condition might not accurately represent the behavior of the fluid near the boundary. In such cases, partial slip or slip boundary conditions become more relevant as they take into account the slip between the fluid and the boundary. This study offers the presentation of numerical experiments for a 2-dimensional channel flow, through a step Navier-Stokes- ω model at high Reynolds numbers. The slip boundary conditions with friction is used in these numerical tests, namely along the step and on the lower and upper walls. The impact of the friction coefficient on the flow characteristics is illustrated. Especially for large Reynolds numbers, the effect of the friction coefficient on the flow region is examined. In the numerical tests, the Crank-Nicolson method is used for time discretization, while the Galerkin finite element method is applied for space discretization. It can be observed that as the coefficient of friction decreased, the eddies are further away from the step and moved towards the outer flow. In addition, the size of the eddies are larger for small coefficients of friction. For Re = 5000, the reattachment length calculated on a fine mesh at time $T = 50$ is close to the step. For Re = 10000, the reattachment lengths determined for different friction coefficients on both meshes are very similar, with eddies forming just behind the step. Similarly, for Re = 15000 and friction co-efficient, $\beta = 0.0001$, the reattachment lengths calculated on the fine mesh are farther from the step. Conversely, for other values of β , the reattachment lengths are close to the step. The results are explained according to flow physics.

ARTICLE HISTORY

Received : 25th July 2023
 Revised : 03rd May 2024
 Accepted : 10th June 2024
 Published : 28th June 2024

KEYWORDS

Slip boundary conditions
Reattachment length
Turbulence
Friction coefficient
Navier-Stokes- ω model

1. INTRODUCTION

The no-slip boundary condition is a boundary condition (BC) that is widely used for convenient fluid velocities and stresses. This condition guarantees that the fluid sticks to the boundary of the flow region. The mathematical simplicity of this condition renders it advantageous compared to partial slip laws. The no-slip BC might not be appropriate for flows characterized by higher Reynolds numbers. As the Reynolds number increases, stress within the system is greater, leading to fluid slipping along the boundary beyond a certain value. Slip is a fluid mechanism that reduces stress. In fluid dynamics, slip refers to a process that minimizes friction or resistance between a fluid and a surface, thereby reducing the stress experienced by the fluid during motion. Slip occurs when the fluid near the boundary moves more freely relative to the surface, reducing the shear stress that would otherwise be caused by the fluid sticking to the surface. This results in lower friction and, consequently, lower stress levels. Therefore, larger Reynolds numbers require a frictional and slip boundary condition for the boundary flows. A turbulence model should be used for numerical solutions of flows with a larger Reynolds number. Large eddy simulation (LES) is the most common turbulence modeling. Furthermore, Leray- α , Navier-Stokes- ω (NS- ω), and NS- α are the other approaches to turbulence models. While modeling the effects of small flow structures on large flow structures, LES also seeks to calculate large eddies of turbulent flows accurately. Galdi and Layton [1] suggest employing frictional slip and no-penetration boundary conditions when dealing with larger eddies. These boundary conditions are more valuable than no-slip BC for describing natural events. For instance, in a hurricane, the main eddies do not adhere closely to the boundary. Hence, the no-slip BC is not suitable for such situations. These eddies slip along the boundary, dissipate energy in the process, and are incapable of penetrating it.

Navier [2] has suggested a partial slip with linear friction boundary condition. When the resistance force on the wall presses against the fluid, slipping occurs in the opposite direction. Furthermore, there exists a linear resistance against to slip. In cases where the coefficient of friction depends on the thermodynamic variables (except at low pressures, especially for the coefficient of friction $\beta = \infty$, the slip boundary condition with linear friction can even account for adhesion [3]. Duhem initially examined the no-slip BC [4,5], later this condition was reviewed by Oseen [6]. In the context of Duhem's boundary conditions (applied to one side of the channel flow where the fluid moves at a constant velocity), the fluid adheres to the wall when the coefficient of friction exceeds a predetermined multiple of the wall's velocity, and vice versa. Noaillon [7] initially proposed a resistance theory incorporating velocity-dependent kinematic viscosity and thermal

conductivity. For situations with low tangential stresses and elevated pressures, this boundary condition indicates adherence. Additionally, frictional slip is transformed into boundary conditions applicable to opposing edges. Clopeou et al. [8] and Coron [9] have investigated the time-dependent NS equations analytically using Navier's slip boundary conditions. Their studies revealed the existence of smooth solutions of 2D Navier-Stokes equations (NSE) with friction boundary conditions and the uniqueness of solutions of 2D NSEs with Navier slip boundary conditions, respectively.

The frictional-slip boundary condition is encountered in many natural events. However, despite this fact, there are few studies on this subject. Therefore, using these boundary conditions in well-defined benchmark problems is essential. In this study, it is preferred to study the flow passing through a step. This is because the recirculation of a flow is a natural phenomenon. The applications of such flows can be observed in wind engineering and various fluid devices, including dams, engine pipes (combustion ducts), turbo machinery and gas turbines [10]. The NS- ω model has been studied by Fan and Zhou [11]. They have shown a unique local solution for the NS- ω model. Layton has proven the existence and regularity of a spherical attractor for this model [12]. Fan et al. have created the global well-posedness of this model by using specific initial data [13]. Recently, Aggul et al. [14] proposed a method that merges the NS-turbulence model through partitioning. Also, Bose and Moin [15] have investigated the wall-bounded LES. They used a dynamic slip boundary condition in the study. Furthermore, Boström [16] has improved the boundary conditions for the simulations of atmospheric boundary layers. Cao [17] also examined the barotropic compressible NSEs with the Navier-type boundary condition in a two-dimensional bounded domain. İlhan and Sahin have presented a study for the Leray- α model. They used the same boundary conditions and examined the effect of friction coefficient on reattachment lengths in their study [18]. Recently, Bermudez et al. [19] proposed and analyzed a mixed variational formulation for the NSEs with variable viscosity that depends nonlinearly on the velocity gradient. Also, Gamar et al. [20] aim to determine how thermal radiation and slip effects affect the flow of a micropolar nanofluid near a stagnation point over an extending sheet. The recent studies have focused on the near wall model [21-23]. There is a significant interest in slip boundary condition research nowadays [24-26].

The aim of this study is to investigate the impact of the friction coefficient on flow characteristics. Slip boundary condition with friction cause the tangential velocity to not reach zero at the upper and bottom boundaries. As a result, the reattachment length is determined by the point where the sign of the tangential velocity changes. A 2-dimensional channel flow through a step is considered. The goal is to determine the reattachment lengths of the recirculation vortices generated behind the step. This study has been prepared as follows: Section 2 presents the description of NS- ω model with slip and friction boundary conditions. The discretization and method as well as the test problem are also described in this section. As a test problem, 2-dimensional channel flows across a step are considered. Section 3 discusses and interprets the numerical results of this test problem. The findings of the study are concluded in Section 4.

2. MATERIALS AND METHODS

2.1 The NS- ω Model with Slip and Friction Boundary Conditions

NS- ω model is a turbulence flow model. This model is an advanced version of the Navier-Stokes equations utilized in computational fluid dynamics. It introduces an additional transport equation for the dissipation rate of turbulent kinetic energy. It is especially valuable in the simulation of turbulent flows, where precise prediction of turbulence characteristics is essential. Also, it is extensively applied in industrial fields such as aerodynamics, heat transfer, and environmental engineering, where turbulence plays a critical role. Let's assume that $\Omega \subseteq \mathbb{R}^d$ ($d = 2$ or 3) domain has boundary to $\partial\Omega$. $\partial\Omega$ boundary consists of three sections: Dirichlet Γ_{diri} , outflow Γ_{out} , and slip-with friction boundary condition Γ_{swf} . $\partial\Omega$ consists of an outward unit normal vector, an orthonormal system of $\{\tau_1, \tau_2, \dots, \tau_{d-1}\}$ tangent vectors and β is the friction coefficient. NS- ω model with the specified boundaries is as follows:

$$u_t - u \times (\nabla \times \bar{u}) + \nabla p - \nu \Delta u = f \text{ in } [0, T] \times \Omega \tag{1}$$

$$\nabla \cdot \bar{u} = 0 \text{ in } [0, T] \times \Omega \tag{2}$$

$$u(0, \cdot) = u_0 \text{ in } \Omega \tag{3}$$

$$u = g \text{ on } [0, T] \times \Gamma_{diri} \tag{4}$$

$$S(u, p)n = 0 \text{ on } [0, T] \times \Gamma_{out} \tag{5}$$

$$\bar{u} \cdot n = 0 \text{ on } [0, T] \times \Gamma_{swf} \tag{6}$$

$$\beta \bar{u} \cdot \tau_i + 2Re^{-1}n \cdot D(\bar{u}) \cdot \tau_i = 0 \text{ on } [0, T] \times \Gamma_{swf} \tag{7}$$

$$u: [0, T] \times \Omega \rightarrow \mathbb{R}^d \tag{8}$$

where, $u: [0, T] \times \Omega \rightarrow \mathbb{R}^d$ is the velocity, $p: [0, T] \times \Omega \rightarrow \mathbb{R}$ is the pressure, u_0 is the initial velocity, T is the final time, and Re is the Reynolds number. $S(u, p)$ is defined as follows:

$$S(u; p) = 2Re^{-1}D(u) - pI \tag{9}$$

In this Eq. (9), I is the unit tensor and $D(u)$ is the velocity deformation tensor,

$$D(u) = \frac{\nabla u + (\nabla u)^T}{2} \tag{10}$$

where, β friction coefficient is a positive function, and it has been calculated by John et al. [27] and İlhan and Sahin [18, 28, 29]. β has been taken as a constant in the calculations. τ_i , ($1 \leq i \leq d - 1$) tangent vectors are selected such that they are from orthonormal bases at 2D ($\{n, \tau_1\}$). In Γ_{swf} boundary condition, $\beta \rightarrow 0$ limit denotes the free-slip, and $\beta \rightarrow \infty$ limit indicates the no-slip.

2.2 Space and Time Discretization

In the NS- ω model simulations, the Crank-Nicolson and Galerkin finite elements method has been used for time and space discretization, respectively. First of all, the grad-div stabilization term and nonlinear scheme for this model are given as follows [30]:

$$\frac{1}{\Delta t}(u_h^{n+1} - u_h^n, v_h) - \left(u_h^{n+\frac{1}{2}} \times \left(\nabla \times w_h^{n+\frac{1}{2}} \right), v_h \right) + \left(p_h^{n+\frac{1}{2}}, \nabla \cdot v_h \right) + \nu \left(\nabla u_h^{n+\frac{1}{2}}, \nabla v_h \right) = f \left(t^{n+\frac{1}{2}} \right) \quad \forall v_h \in X_h \tag{11}$$

$$\left(\nabla \cdot u_h^{n+\frac{1}{2}}, q_h \right) = 0, \quad \forall q_h \in Q_h \tag{12}$$

$$(w_h^{n+1}, \chi_h) + \alpha^2 (\nabla w_h^{n+1}, \nabla \chi_h) - (u_h^{n+1}, \chi_h) = 0, \quad \forall \chi_h \in X_h \tag{13}$$

Thus, the above nonlinear scheme gives the following Newton iteration for each time step:

$$\begin{aligned} & \frac{1}{\Delta t}(u_h^{n+1,k}, v_h) - (p_h^{n+1,k}, \nabla \cdot v_h) + \frac{\nu}{2}(\nabla u_h^{n+1,k}, \nabla v_h) - \frac{1}{4}(u_h^{n+1,k} \times (\nabla \times w_h^{n+1,k-1}), v_h) \\ & - \frac{1}{4}(u_h^{n+1,k-1} \times (\nabla \times w_h^{n+1,k}), v_h) + \frac{1}{4}(u_h^{n+1,k-1} \times (\nabla \times w_h^{n+1,k-1}), v_h) \\ & - \frac{1}{4}(u_h^{n,k} \times (\nabla \times w_h^{n+1,k}), v_h) - \frac{1}{4}(u_h^{n+1,k} \times (\nabla \times w_h^{n,k}), v_h) - \frac{1}{4}(u_h^{n,k} \times (\nabla \times w_h^{n,k}), v_h) \\ & = \frac{1}{\Delta t}(u_h^n, v_h) - \frac{\nu}{2}(\nabla u_h^n, \nabla v_h) + \left(f \left(t^{n+\frac{1}{2}} \right), v_h \right), \quad \forall v_h \in X_h \end{aligned} \tag{14}$$

$$(\nabla \cdot u_h^{n+1}, q_h) = 0, \quad \forall q_h \in Q_h \tag{15}$$

$$(w_h^{n+1}, \chi_h) + \alpha^2 (\nabla w_h^{n+1}, \nabla \chi_h) - (u_h^{n+1}, \chi_h) = 0, \quad \forall \chi_h \in X_h \tag{16}$$

This way, grad-div stabilization and Newton iteration is obtained as follows:

$$\begin{aligned} & \frac{1}{\Delta t}(u_h^{n+1,k}, v_h) - (p_h^{n+1,k}, \nabla \cdot v_h) + \frac{\nu}{2}(\nabla u_h^{n+1,k}, \nabla v_h) - \frac{1}{4}(u_h^{n+1,k} \times (\nabla \times w_h^{n+1,k-1}), v_h) \\ & - \frac{1}{4}(u_h^{n+1,k-1} \times (\nabla \times w_h^{n+1,k}), v_h) + \frac{1}{4}(u_h^{n+1,k-1} \times (\nabla \times w_h^{n+1,k-1}), v_h) \\ & - \frac{1}{4}(u_h^{n,k} \times (\nabla \times w_h^{n+1,k}), v_h) - \frac{1}{4}(u_h^{n+1,k} \times (\nabla \times w_h^{n,k}), v_h) \\ & - \frac{1}{4}(u_h^{n,k} \times (\nabla \times w_h^{n,k}), v_h) + \frac{1}{2}(\nabla \cdot u_h^{n+1}, \nabla \cdot v_h) \\ & = \frac{1}{\Delta t}(u_h^n, v_h) - \frac{\nu}{2}(\nabla u_h^n, \nabla v_h) - \frac{1}{2}(\nabla \cdot u_h^n, \nabla \cdot v_h) + \left(f \left(t^{n+\frac{1}{2}} \right), v_h \right), \quad \forall v_h \in X_h \end{aligned} \tag{17}$$

$$(\nabla \cdot u_h^{n+1}, q_h) = 0, \quad \forall q_h \in Q_h \tag{18}$$

$$(w_h^{n+1}, \chi_h) + \alpha^2 (\nabla w_h^{n+1}, \nabla \chi_h) - (u_h^{n+1}, \chi_h) = 0, \quad \forall \chi_h \in X_h \tag{19}$$

Here, the function spaces are as follows for $d = 2, 3$:

$$P_n := \{p: \Omega \rightarrow \mathbb{R}^d\} \tag{20}$$

where, p is the polynomial of degree n . Other function spaces are defined as follows,

$$X_h := \{v_h \in C_0(\Omega), v_h = 0, \text{ on } \partial(\Omega), v_h \in P_2\} \tag{21}$$

$$Q_h := \{q_h \in C_0(\Omega), \int_{\Omega} q_h dx = 0, q_h \in P_1\} \tag{22}$$

In all these simulations, $u_h^{n+1,k}$ is the unknown velocity, $u_h^{n+1,k-1}$ is the velocity solution in the previous iteration, $u_h^{n,k}$ is the velocity solution in the previous time step and v_h is the test function. The time step has been taken as $\Delta t =$

0.1; in other words, 1 second corresponds to 10 iterations. The slip boundary condition with friction can be applied to finite elements code [18, 27-29, 31-33].

2.3 The Numerical Simulations

The forward-backward step problem is of great importance in computational fluid dynamics. There are many test problems in this field, and the most important test problem is the driven cavity model. The definition domain of the problem is a square. While the no-slip BC is applied on all boundaries except the upper boundary of the square, the tangential component of the velocity on the upper wall is taken as constant. Also, the problem is complex since there are non-physical singularities at the corners of the region. The biggest shortcoming of this problem is that it is not physically real. The forward-backward step problem presented in this study is also commonly used. This can be observed in Armaly's studies [33]. Traits such as reattachment length and scaling with Reynolds number simplify this test problem [34]. Gunzburger [35] suggests that flow problems such as flow over a step are better test problems. The reason is that they are geometrically simple. This study examines a flow over a step problem [18, 27, 28, 31, 33, 36]. This study also investigates how the reattachment length of the eddy varies with different friction parameters in two-dimensional flows. The domain is a 40 × 10 channel with a 1 × 1 step extending five units into the channel at the bottom, as shown in Figure 1. The inflow boundary condition on the left side of the channel is defined as

$$u = \left(\frac{y(10 - y)}{25}, 0 \right) \tag{23}$$

The slip and friction boundary condition, defined by Eq. (7), is applied to the upper and bottom boundaries as well as along the step. The goal of the SWF boundary condition is to obtain physically the correct flow behaviors using coarse discretization in space. This helps to create a successful model. The flow leaves the domain with an outflow boundary condition on the right side of the channel.

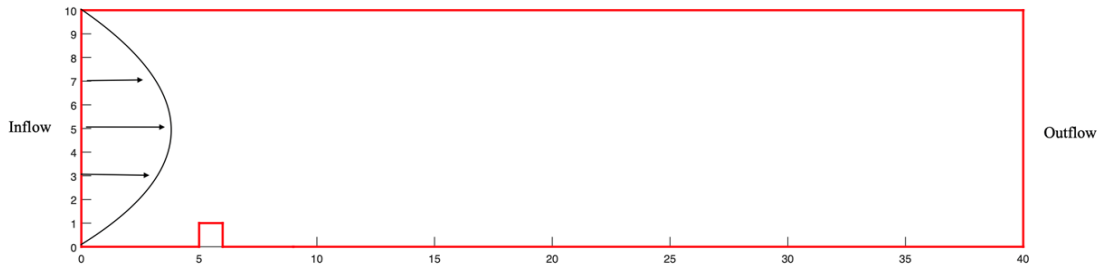
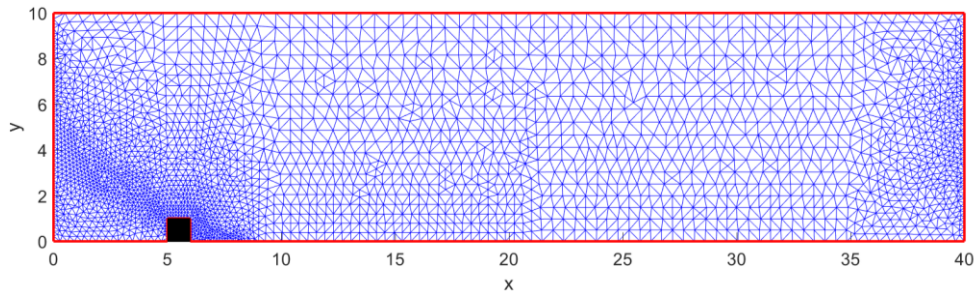
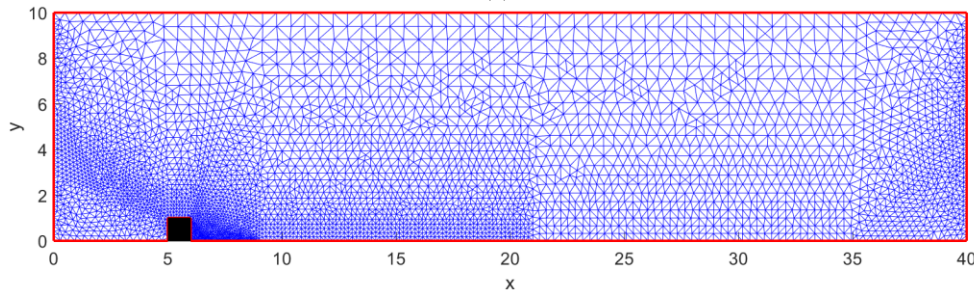


Figure 1. Domain of two-dimensional channel with a step



(a)



(b)

Figure 2. (a) Coarse mesh, level = 3 and (b) fine mesh, level = 4

The aim is to calculate the reattachment lengths of the recirculation vortices formed behind the step. The purpose of this study is to determine the reattachment lengths of the recirculation vortices generated behind the step. Slip boundary condition with friction cause the tangential velocity to not vanish at the upper and bottom boundaries. Therefore, the reattachment length is defined as the place where the sign of the divergent velocity changes. All simulations have been performed using the FreeFEM++ [37] computer program. In the simulations, $\alpha = 1$ is taken. Fine and coarse meshes

have been used for the simulations as shown in Figure 2. The degrees of freedom are 47222 and 19956 for velocity and pressure in fine mesh, respectively, while 30735 and 12951 in coarse mesh. The problem (1-8) can be shortly shown as $NS-\omega + SWF$.

3. RESULTS AND DISCUSSION

Figure 3 indicates that for $Re = 5000$ and $Re = 10000$, respectively, with $\beta = 1$, two eddies form behind the step, and the last eddy is close to the step. Figure 4 shows that for $Re = 5000$ and $\beta = 0.001$, eddies form behind and in front of the step, and the eddies behind the step are close to the step. Similarly, Figure 5 shows that for $\beta = 0.01$ and 10 , an eddy is formed behind the step. This eddy is around the $x = 10$ point. It is seen from Figure 6 for $Re = 10000$ and $\beta = 0.01$ and 1 , two eddies are formed behind the step. The first eddy starts around position $x = 20$, and the second eddy forms around position $x = 7$. For $Re = 15000$ and $\beta = 1$ and 10 , two eddies are developed, the first being around the $x = 20$ position and the second around the $x = 8$ position (see Figure 7).

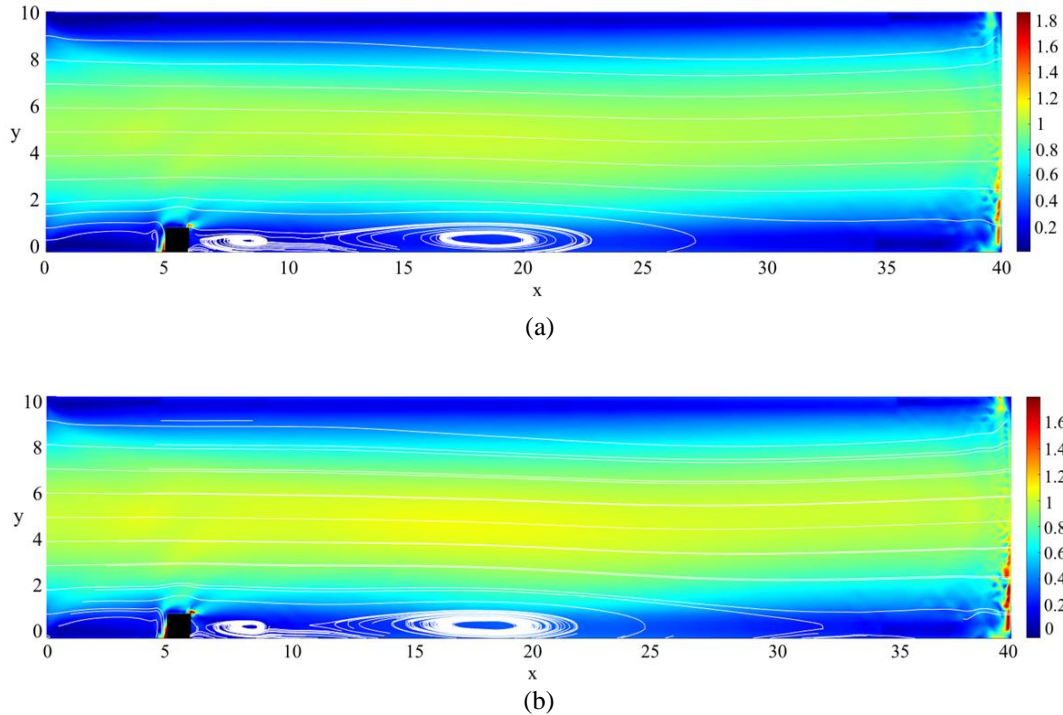


Figure 3. Streamlines over velocity contours on coarse mesh (level = 3), at time $T = 50$, for $\beta = 1$, (a) $Re = 5000$ and (b) $Re = 10000$

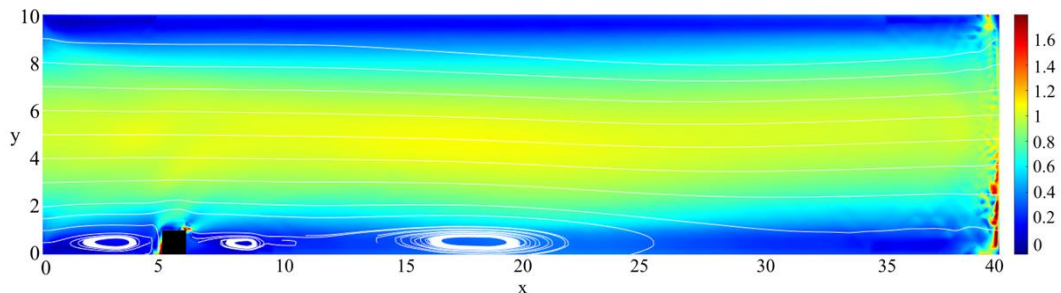


Figure 4. Streamlines over velocity contours on coarse mesh (level = 3), at time $T = 50$, for $\beta = 0.001$, $Re = 5000$

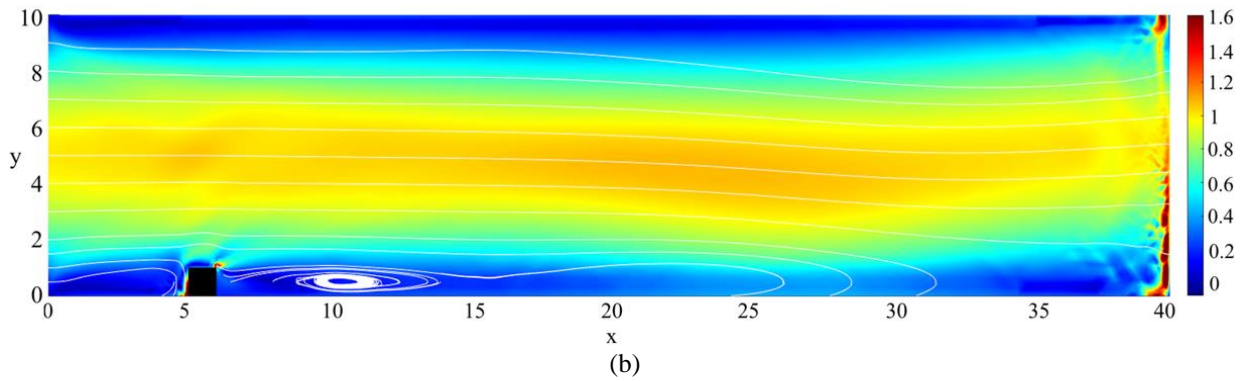
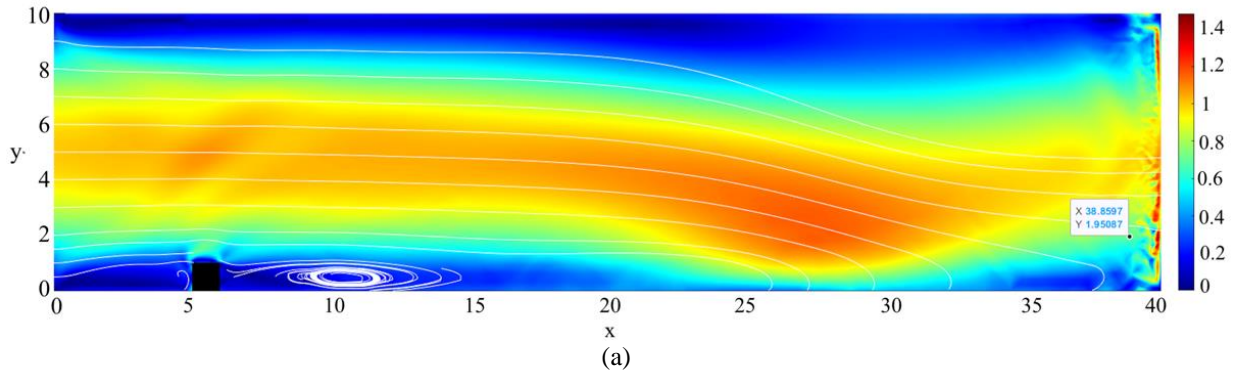


Figure 5. Streamlines over velocity contours on coarse mesh (level = 3) at time $T = 50$ and $Re = 5000$ (a) $\beta = 0.01$ and (b) $\beta = 10$

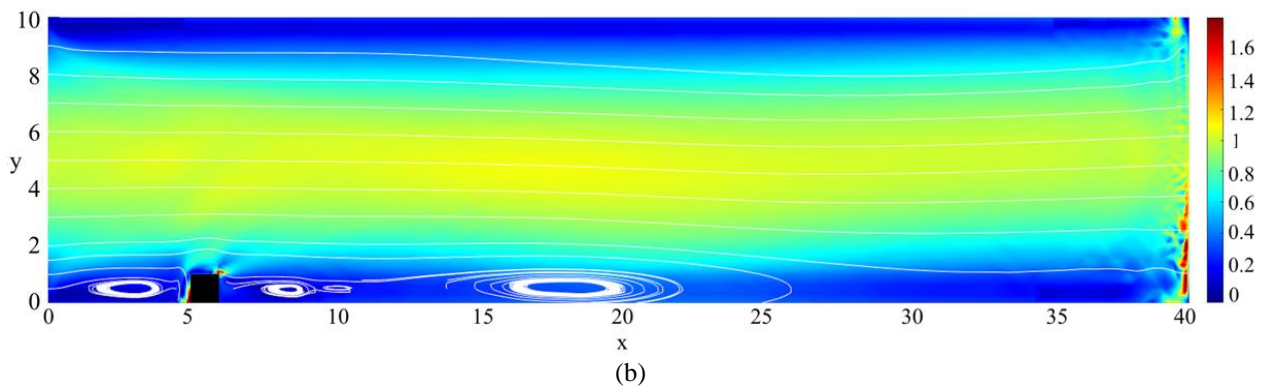
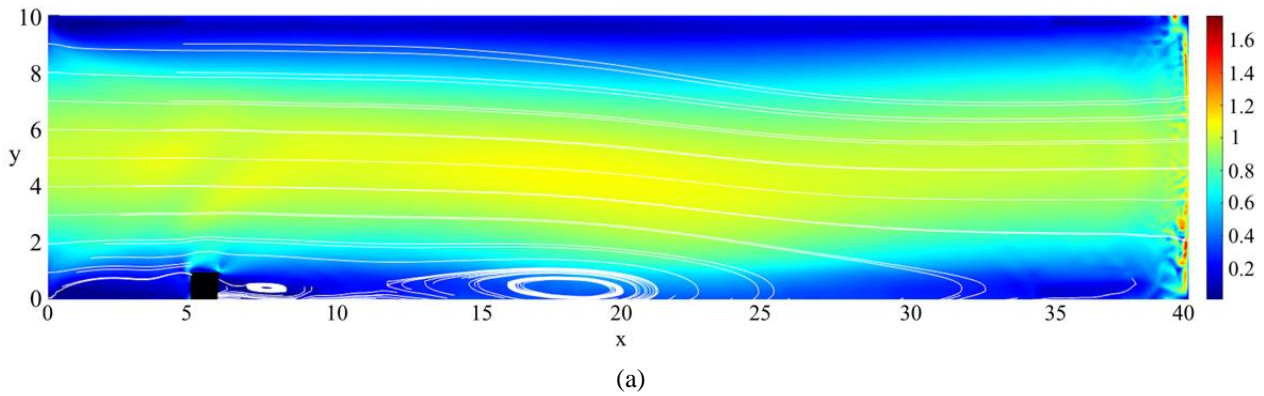


Figure 6. Streamlines over velocity contours on coarse mesh (level = 3), at time $T = 50$, $Re = 10000$ (a) $\beta = 0.01$ and (b) $\beta = 10$

It can be seen from Figure 8 that for $Re = 5000$ and all β values, the calculated reattachment length on fine mesh and at time $T = 50$ is near to the step. For $Re = 10000$, the reattachment lengths calculated for distinct friction coefficients in both meshes are very near to each other, and the eddies form just behind the step (see Figure 9). It can be induced from Figure 10 that for $Re = 15000$ and $\beta = 0.0001$, the calculated reattachment lengths in the fine mesh are away from the step. For the other values of β , the reattachment lengths are near to the step. At $T = 50$ and coarse mesh,

as the friction coefficient decreases, the reattachment lengths move away from the step. At $T = 50$ and fine mesh, the reattachment lengths are approximately the same as shown in Figures 8-10. Moreover, it can be seen in Figures 8-10 that the reattachment lengths computed for all Reynolds numbers and small friction coefficients are larger than those calculated for significant friction coefficients at time $T = 50$. So, it can be said that for small friction coefficients, the position of the reattachment lengths moves towards the outflow, and conversely, for the large friction coefficients, reattachment lengths occur near the behind of the step.

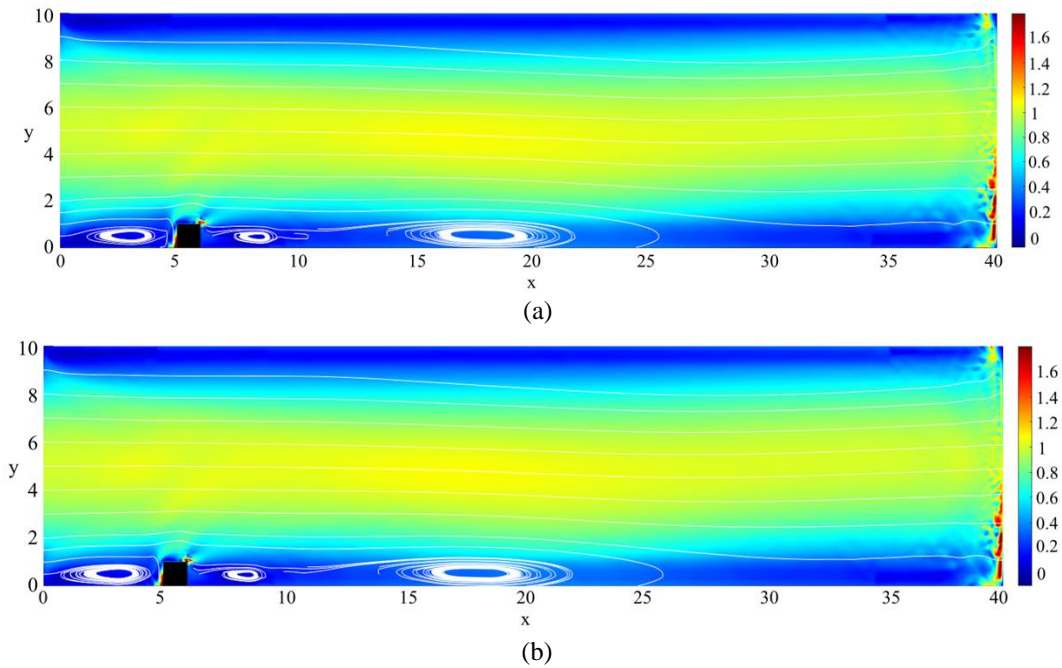


Figure 7. Streamlines over velocity contours on coarse mesh (level = 3), at time $T = 50$, $Re = 15000$ (a) $\beta = 1$ and (b) $\beta = 10$

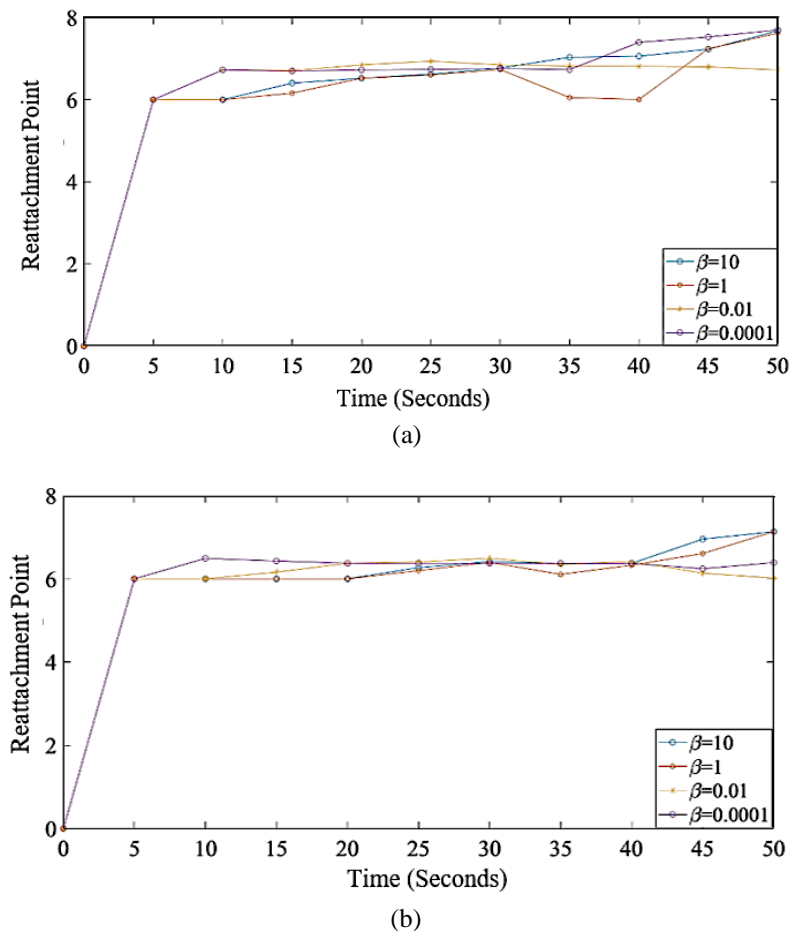


Figure 8. Reattachment lengths and time, for $Re = 5000$ (a) level = 3 and (b) level = 4

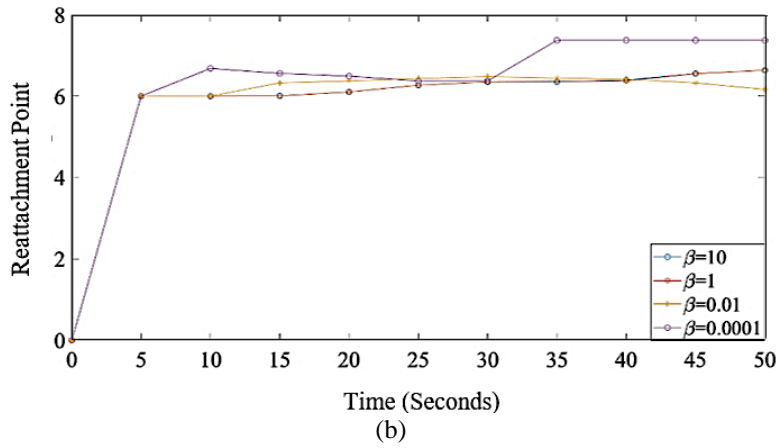
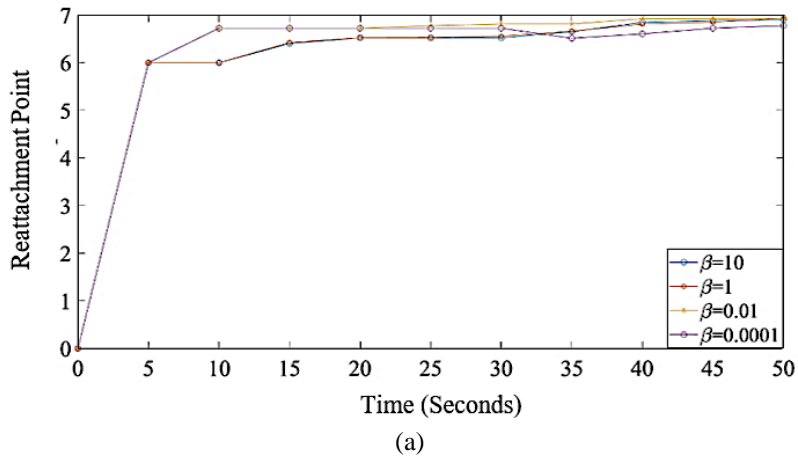


Figure 9. Reattachment lengths and time for $Re = 10000$ (a) level = 3 and (b) level = 4

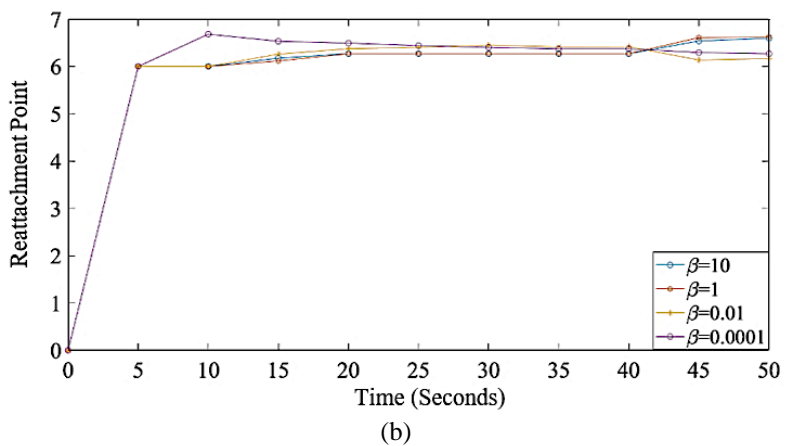
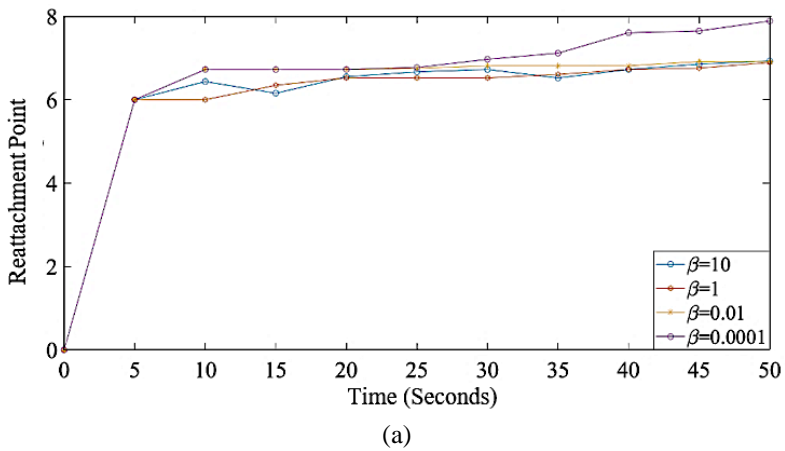


Figure 10. Reattachment lengths and time, for $Re = 15000$ (a) level = 3 and (b) level = 4

The eddies formed in the simulations obtained using the small Reynolds number and the large friction coefficient are smaller. Regarding all Reynolds numbers, the reattachment lengths in simulations using fine mesh are smaller and the eddies are around point $x = 7$ (see Figures 8(b), 9(b), and 10(b)). Conversely, simulations using coarse mesh have larger reattachment lengths as shown in Figures 8(a), 9(a), and 10(a). In other words, the eddies are around the $x = 8$ point. İlhan and Sahin [18] used the logarithmic law to calculate the friction coefficients. They computed the reattachment lengths for calculated and different friction coefficients. Moreover, simulations of NS- ω and Leray- α models were performed using the same meshes for different Reynolds numbers. The reattachment lengths obtained with the Leray- α model are greater than those obtained with the NS- ω model; that is, recirculating vortices form away from the step. For Reynolds numbers of 50 and 100, numerical investigations were conducted on slip with friction boundary conditions for a steady 2-D flow over a step and under a constant inflow profile [31]. In both simulations, as friction decreased, the reattachment length of the eddies shifted further downstream. The reattachment points obtained for the friction parameter $\beta = 10$ are similar to those obtained with the no-slip BC. Similar result is also observed in this study. In a similar study presented for Reynolds number $Re = 500$ and different beta friction parameters for the NSE, it was observed that as the friction parameter decreased, the reattachment point continued to move downstream, but without the formation of a new vortex, across all grids [32]. For $\beta = 1$, it is noticeable that the vortex detaches from the lower boundary around $x = 20$ and then reattaches slightly downstream. Similar results have been obtained in this study as well. Similarities are observed between the study conducted by İlhan [29, 38] and this study. In both investigations, it was discovered that with the rise in friction coefficient across all grids employed in simulations, both the reattachment length and the size of the recirculating vortex diminish. Additionally, eddies tend to form close to the step at high Reynolds numbers.

4. CONCLUSIONS

In this study, the slip boundary conditions with friction have been applied to the NS- ω turbulence model, and the flow behaviours over a whole step in 2D have been analysed. The main purpose in doing so is to reveal the impact of friction coefficient on flow behaviour. The results of the numerical simulations were compared for $\beta = 0.0001, 0.01, 1$, and 10 on the coarse and fine mesh by taking Reynolds numbers $Re = 5000, 10000$, and 15000 . Eddies mainly were formed behind the step, but in some cases, eddies were also formed in the front of the step. As the coefficient of friction decreased (i.e., $\beta \rightarrow 0$), the eddies were further away from the step and moved towards the outer flow. In addition, the dimensions of the eddies are larger for small coefficients of friction. The eddies not only provide transport but also, when the coefficient of friction changes, the eddies form, penetrating into the flow according to the velocity magnitude varying at the boundary. This movement is seen in all flows' bottom wall and centre plane. This supports the claim that the study is compatible with the physics of the flow. In future studies, this problem will be applied to 3D flows.

ACKNOWLEDGEMENTS

This study was not supported by any grants from funding bodies in the public, private, or not-for-profit sectors.

CONFLICT OF INTEREST

The authors declare no conflicts of interest.

AUTHORS CONTRIBUTION

Ö. İlhan (Conceptualization; Formal analysis; Visualisation; Methodology; Data curation; Writing - original draft; Resources)

REFERENCES

- [1] G. P. Galdi and W. J. Layton, "Approximation of the larger eddies in fluid motion II: A model for space filtered flow," *Mathematical Models and Methods in Applied Sciences*, vol. 10, no. 3, pp. 343-350, 2000.
- [2] C. M. L. H. Navier, "Sur les lois de l'équilibre et du mouvement des corps élastiques," *Memoires de l'Academie des Sciences de l'Institut de France*, vol. 6, pp. 389-441, 1827.
- [3] J. Serrin, "Mathematical principles of classical fluid mechanics," *Encyclopedia of Physics*, vol. 3/8/1, pp. 125-263, 1959.
- [4] P. Duhem, "On the boundary conditions in hydrodynamics," *Comptes Rendus*, vol. 134, pp. 149-151, 1902.
- [5] P. Duhem, "On certain cases of adherence of a viscous liquid to solids immersed in it," *Comptes Rendus*, vol. 134, pp. 265-267, 1902.
- [6] C. W. Oseen, "Contributions to hydrodynamics," *Annalen der Physik*, vol. 46, pp. 231-252, 1915.
- [7] P. Noaillon, "Attempt at a new theory of the resistance of fluids," *Comptes Rendus*, vol. 188, pp. 441-443, 1929.
- [8] T. Clopeau, A. Mikelić and R. Robert, "On the vanishing viscosity limit for the 2D incompressible Navier-Stokes equations with the friction type boundary conditions," *Nonlinearity*, vol. 11, no. 6, pp. 1625-1636, 1998.

- [9] J. M. Coron, "On the controllability of the 2-D incompressible Navier- Stokes equations with the Navier slip boundary conditions," *ESAIM Controle Optimisation and Calculus of Variations*, vol. 1, pp. 35-75, 1996.
- [10] R. R. Hwang, Y. C. Chow and Y. F. Peng, "Numerical study of turbulent flow over two-dimensional surface-mounted ribs in a channel," *International Journal for Numerical Methods in Fluids*, vol. 31, pp. 767-785, 1999.
- [11] J. Fan and Y. Zhou, "Global well-posedness of the Navier- Stokes- ω equations," *Applied Mathematics Letter*, vol. 11, no. 24, pp. 1915-1918, 2011.
- [12] W. J. Layton, 'Existence of smooth attractors for the Navier-Stokes- ω model of turbulence' *Journal of Mathematical Analysis and Applications*, vol. 366, no. 1, pp. 81-89, 2010.
- [13] J. Fan, F. Li and G. Nakamura, "Global solutions to the Navier-Stokes- ω and related models with rough initial data," *Zeitschrift für angewandte Mathematik und Physik*, vol. 65, pp. 301-314, 2014.
- [14] M. Aggul, A. E. Labovsky and K. J. Schwiebert, "NS- ω model for fluid-fluid interaction problems at high Reynolds numbers," *Computer Methods in Applied Mechanics and Engineering*, vol. 395, p. 115052, 2022.
- [15] S. T. Bose and P. Moin, "A dynamic slip boundary condition for wall-modeled large-eddy simulation," *Physics of Fluids*, vol. 26, no. 1, p. 015104, 2014.
- [16] E. Bostrom, "Boundary conditions for spectral simulations of atmospheric boundary layers," *Ph.D. Thesis*, Royal Institute of Technology, Stockholm, Sweden, 2017.
- [17] Y. Cao, "Global classical solutions to the compressible Navier-Stokes equations with Navier-type slip boundary condition in 2D bounded domains' *Journal of Mathematical Physics*, vol. 64, p. 111506, 2023.
- [18] Ö. İlhan and N. Şahin, "Testing of logarithmic law for the slip with friction boundary condition," *International Journal of Nonlinear Sciences and Simulation*, vol. 24, no. 8, pp. 2823-2837, 2024.
- [19] I. Bermúdez, C. I. Correa, G. N. Gatica and J. P. Silva, "A perturbed twofold saddle point-based mixed finite element method for the Navier-Stokes equations with variable viscosity," *Applied Numerical Mathematics*, vol. 201, pp. 465-487, 2024.
- [20] F. Gamar, M. D. Shamsuddin, M. S. Ram, S. O. Salawu and E. O. Fatunmbi, "Exploration of thermal radiation and stagnation point in MHD micropolar nanofluid flow over a stretching sheet with Navier slip," *Numerical Heat Transfer, Part A: Applications*, vol. 85, no. 15. pp. 1–13, 2024.
- [21] S. G. Cai, J. Jacob and P. Sagaut, "Immersed boundary based near-wall modeling for large eddy simulation of turbulent wall-bounded flow," *Computers & Fluids*, vol. 259, p. 105893, 2023.
- [22] S. Lyu and S. Utyuzhnikov, "A computational slip boundary condition for near-wall turbulence modelling," *Computers & Fluids*, vol. 246, pp. 105628, 2022.
- [23] H. Maeyama, T. Imamura, J. Osaka and N. Kurimoto, "Turbulent channel flow simulations using the lattice Boltzmann method with near-wall modeling on a non-body-fitted Cartesian grid," *Computers & Mathematics with Applications*, vol. 93, pp. 20-31, 2021.
- [24] Z. Li, X. Pan and J. Yang, 'Constrained large solutions to Leray's problem in a distorted strip with the Navier-slip boundary condition,' *Journal of Differential Equations*, vol. 377, pp. 221-270, 2023.
- [25] F. Wang, M. Ling, W. Han and F. Jing, "Adaptive discontinuous Galerkin methods for solving an incompressible Stokes flow problem with slip boundary condition of frictional type," *Journal of Computational and Applied Mathematics*, vol. 371, p. 112700, 2020.
- [26] J. K. Djoko, J. Koko, M. Mbhou and T. Sayah, "Stokes and Navier-Stokes equations under power law slip boundary condition: Numerical analysis," *Computers & Mathematics with Applications*, vol. 128, pp. 198-213, 2022.
- [27] V. John, W. Layton and N. Sahin, "Derivation and analysis of near-wall models for channel and recirculating flows," *Computers & Mathematics with Applications*, vol. 28, pp. 1135-1151, 2004.
- [28] N. Sahin, "Derivation, analysis and testing of new near wall models for large eddy simulation," *Ph.D. Thesis*, Pittsburgh University, United States, 2003.
- [29] Ö. İlhan, "Slip with friction boundary conditions for the Navier–Stokes-alpha turbulence model and the effects of the friction on the reattachment point," *International Journal of Non-Linear Mechanics*, vol. 159, p. 104614, 2024.
- [30] R. G. Hill, "Benchmark testing the α -models of turbulence," *Master Thesis*, Clemson University, United States, 2010.
- [31] V. John, "Slip with friction and penetration with resistance boundary conditions for the Navier-Stokes equations: Numerical tests and aspects of the implementation," *Journal of Computational and Applied Mathematics*, vol. 147, pp. 287-300, 2002.
- [32] V. John and A. Liakos, "Time-dependent flow across a step: the slip with friction boundary condition," *International Journal for Numerical Methods in Fluids*, vol. 50, 713-731, 2006.

- [33] B. F. Armaly, F. Durst, J. C. F. Pereira and B. Schönung, “Experimental and theoretical investigation of backward-facing step flow,” *Journal of Fluid Mechanics*, vol. 127, pp. 473-496, 1983.
- [34] A. Halim and M. Hafez, ‘Calculation of separation bubbles using boundary layer type equations,’ *Computational Methods in Viscous Flows*, vol. 3, pp. 395-415, 1984.
- [35] M. D. Gunzburger. Finite Element Methods for Viscous Incompressible Flows: A Guide to Theory, Practice, and Algorithms, 1st ed. New York: Academic Press, 1989.
- [36] I. Moulinos, C. Manopoulos and S. Tsangaris, “Computational analysis of active and passive flow control for backward facing step,” *Computation*, vol. 10, no. 1, pp.12, 2022.
- [37] F. Hecht, FreeFEM Documentation (Release 4.13), pp. 1-740, 2024.
- [38] Ö. İlhan, “Application of a near wall model to Navier-Stokes equations with nonlinear time-relaxation model,” *Journal of Applied Mathematics and Computational Mechanics*, vol. 21, no. 2, pp. 39-50 2022.

NOMENCLATURE

Symbol			
u	Velocity of fluid	β	Friction coefficient
p	Pressure of fluid	τ_i	Tangent vectors
u_0	Initial velocity	n	Unit normal vector
T	Final time (second)	Γ_{diri}	Dirichlet boundary condition
Re	Reynolds number	Γ_{out}	Outflow boundary condition
$S(u, p)$	Stress tensor	Γ_{swf}	Slip-with friction boundary condition
$D(u)$	Velocity deformation tensor	$u_h^{n+1,k}$	Unknown velocity
Ω	Domain (unit square)	$u_h^{n+1,k-1}$	Velocity solution in the previous iteration
$\partial\Omega$	Boundary of domain (unit)	$u_h^{n,k}$	Velocity solution in the previous time step
I	Unit tensor	Δt	Time step (second)

Abbreviations

NSE	Navier-Stokes Equations,
SWF	Slip with Friction
No-slip BC	No-slip Boundary Condition
NS- ω	Navier-Stokes- ω
NS- α	Navier-Stokes- α
LES	Large Eddy Simulation